YIELD STRESS VARIATION ACROSS THICKNESS FOR STEEL (HC SS316) SPECIMEN HOT ROLLED AT LOW REDUCTION AND LOW STRAIN RATES

P. O. AIYEDUN

Present Address and Address for Correspondence:
Department of Mechanical Engineering
University of Ibadan, Ibadan, Nigeria.

ABSTRACT

For the hot flat rolling of HC SS316 at low reduction (r ~10%) and low strain rates ($\bar{\varepsilon}$ ~0.08 s^{-1}), a new method of estimating the material mean yield strength ($\bar{\sigma}_g$ *) is hereby proposed. It combines the temperature, strain, as well as the composition effects and was obtained from equations based on hot torsion isothermal tests under similar conditions.

The surface third element across thickness has a strain increase of ~15% increase of ~1 x 10^4 in the Zener- Hollomon parameter, Z value and a decrease of ~ 250°C in the rolling temperature ($\bar{T}_m$). This corresponded to an increase of ~200Nmm^{-2} in the yield strength of the surface element and an increase of ~35% in the material mean yield strength $\bar{\sigma}_g$ * (YKP or YKG). This was found to be due to the temperature, composition and rolling condition effects.

An almost 3 times increase in the yield strength of the surface material compared to the centre material confirm the reverse sandwich (or rolling chilling) effect for hot flat rolling at low strain rates.

INTRODUCTION

The flow stress of a metal is influenced by:

(1) Factors unrelated to the deformation process such as chemical composition, metallurgical structure, phases, grain size, segregation, prior strain history.

(2) Factors explicitly related to the deformation process: Temperature of deformation, degree of deformation and rate of deformation. Altan and Boulger, (1973), Venter and Abd-Rabbo (1980).

At high temperatures, flow stress of metals and alloys is complicated, two opposing tendencies viz, workhardening and recovery or recrystallization compete simultaneously: Suzuki, et al. (1968).

For hot rolling at low strain rates, "roll chilling" effect reduces the bulk mean temperature in the roll gap and increases the resistance to deformation. It also has a second effect called "reverse sandwich effect" upon the metal in the roll gap. The soft metal core with hard chilled surface material, rolls with a resistance to deformation which approaches the resistance to deformation of the metal at the surface temperature. Sparling (1983), Aiyedun (1984).

The appropriate temperature for the evaluation of the mean resistance thus some value which is weighted in favour of the surface temperature.

Rolling loads and torques are dependent on the following factors:

-Geometry of rolling process

- yield stress, strain rate
- rolling temperature
- friction, and spread

The yield stress in turn depends on current strain, strain rate and temperature of rolling.

$$\bar{k}_p = \frac{1}{\alpha}\int_0^{\alpha} k\,d\theta \qquad (1)$$

$$\bar{k}_g = \frac{1}{\gamma}\int_0^{\gamma} k\,de = \frac{2}{\alpha^2}\int_0^{\alpha} k\theta\,d\theta \qquad (2)$$

where $e = \frac{h_o - h}{h_o}$

Replacing k by $\bar{k}$ (mean yield stress) shows a < 2% and ≤ 10% effect on rolling load and torque.

These mean yield stresses, $\bar{k}$, are obtained experimentally by torsion or plane strain compression under similar conditions of ε, $\dot{\varepsilon}$, and T as for the hot flat rolling schedules of interest.

The two main hot working tests used to determine the resistance to deformation are:

(i) Scaled down test such as rolling, extrusion, forging, etc. where the variable inherent in the material e.g. composition, size, shape, structure, strain rate, lubrication, temperature and stress system are simultaneously covered.

(ii) Mechanical tests viz tension, compression, torsion and bending. Tension, compression and torsion have all been adapted for high temperature deformation.

In the plane strain compression test, a strip sample is compressed between two flat narrow plattens which overlap the edges of the sample. Servo hydraulic systems have been used to obtain constant true strain rates in a plane compression machine (Sellars, et al; 1976). Multipass rolling schedule and constantly varying strain rates during a rolling pass have also been simulated (Sellar et al; 1976).

Hot torsion testing in which a twisting moment is applied to a solid or tubular sample has been accepted worldwide. At strain rates of (10^{-3} to 10^{2} s^{-1}) measurement of flow stress and ductility are obtained.

The specimen geometry is kept constant by constraining them axially (Barraclough, 1974; Sah, 1970).

In this work, hot torsion testing has been used to obtain the strength of SS316 for strain rates of interest, (0.01 - 1.5 s^{-1}) and temperature range of (600 - 1200°C) at constant strain rate (Aiyedun, 1984).

EXPERIMENTAL METHODS

For the determination of the Hot Strength of HC SS316 (i.e. stress-strain equations) torsion tests were carried out at various constant temperatures of 600, 805, 900, 1000, 1098 and 1200°C and at different equivalent tensile strain rates of 0.0036, 0.029, 0.360 and 1.400 s^{-1} in an argon atmosphere. A gauge/radius ratio of 4 was chosen and torsion specimens of 14.00mm gauge length and 7.00mm gauge diameter were machined from heat treated slabs of HC SS316. A summary of the general description and the technical data of the torsion machine used is given by Cole (1979).

All tests were performed under the condition of "fixed end" i.e. specimen diameter held constant to prevent extension or contraction of gauge length during deformation. Temperature was measured using a Pt - Pt/13%Rh thermocouple inserted to within 1mm of end of gauge length of specimen shoulder, connected to a potentiometer recorder. All test data, torque "r", angle of twist, θ were continously traced on an ultra-violet recorder.

The true stress, σ, true strain, ε, and true strain rate, $\dot{\varepsilon}$, at the effective radius were obtained by the following equations:

$$\sigma = \sqrt{3}.\gamma = \frac{3\sqrt{3}.\Gamma}{2\pi r^3} \quad (3)$$

$$\varepsilon = \frac{\gamma}{\sqrt{3}} = \frac{a.\theta}{\sqrt{3}.l} \quad (4)$$

$$\dot{\varepsilon} = \frac{\dot{\gamma}}{\sqrt{3}} = \frac{a.\dot{\theta}}{\sqrt{3}.l} \quad (5)$$

where Γ Torque; r - specimen radius; a = 0.724 r i. e. effective radius): l - gauge length; θ and $\dot{\theta}$* are angle of twist (radians) and twisting speed (radians/s)

By using equations (3) - (5), raw experimental torsion data were converted to stress, strain, and strain rate. The data were then plotted into stress-strain curves at various strain rates and temperatures. See Fig. 4a -4d.

A specimen (SP PN1) was hot rolled at a low reduction (r ~ 10%) and low strain rate ($\dot{\bar{\varepsilon}} \sim 0.08$ s^{-1}). Rolling data, Viz strain, strain rate, rolling temperature were obtained for various times during roll contact and for the complete half profile as well as for zones a, b, and c that the half profile was subdivided into as given in tables 2-6.

Plots of $\dot{\bar{\varepsilon}}$ vs ε, T vs ε, Z vs ε, σ - ε curve for variable Z and for $\bar{Z}$ for SP PNI are given in figures (1), 2a and 2b, while the strain profile across thickness and their corresponding temperature profile for zones a, b, and c are given in figures 7a and 7b.

STRESS-STRAIN BEHAVIOUR

For SS316, increasing strain, ε , the equivalent stress, $\bar{\sigma}$ increases during the initial work hardening stage to a maximum value and then falls to a steady-state flow stress. The stress at a given strain, and the strain to the peak stress, ε_p, increase with increasing strain rate and decreasing temperature.

Discrepancies in absolute values of flow stress under similar testing methods by different workers indicate the importance of matrial factors such as composition and structure before test, and their changes during testing (see fig. 6a and 6b).

Yield strength of a material depends on the material composition, the thermomechanical history before working (Roberts, 1978), method and circumstances of its measurement e.g. temperature sensitivity of yield strength of alloys differing from that of the parent metal due to atomic rearrangements or phase transformation occuring as the temperature is raised. These effects influence interaction between dislocations and the solute atoms or alter the amount and/or dispersion of a second phase. The work hardening effect (increase in yield stress with increasing strain) increase with increasing strain rate.

Zener and Hollomon (1944) proposed an equation combining the simultaneous effect of strain rate and temperature on yield stress.

$$\sigma = f(\varepsilon \exp {}^{Q}/_{RT}) = f(Z) \quad (6)$$

The hot strength of SS316 was thus expressed in algebraic equations and plotted in terms of σ^* vs $\log_{10}Z$ to cover the temperature range (600 - 1200°C) and the strain rate of interest (0.004 - 1.4) s^{-1} where $\sigma^* = \sigma_p, \sigma_o, \sigma_{0.1}, \sigma_{ss}$ after due consideration of the earlier thermo-mechanical history of the material.

Higher solution treatment temperatures and higher carbon content lead to faster precipitation of carbides and nitrides in steels. With the presence of Nb, V, and T in our stainless steel of interest (SS316), there is possibility of the formation of their precipitates either dynamically or statically during their deformation at low strain rates. This will influence the dynamic recovery and recrystallisation rates and hence the hot strength.

EFFECTS OF COMPOSITION ON THE HOT STRENGTH OF STEEL

Alloying elements in steel can alter the hot strength of austenite by either:

(1) Solid solution strengthening i.e. elements dissolving interstitially or substitutionally to form single phase solid solutions.

(2) Precipitation hardening i.e. elements combining with carbon or nitrogen to form precipitates.

According to Tegart and Gittins, (1976) and Sage (1979) alloying elements which strengthen austenite act independently of each other i.e. niobium and vanadium both have an additive effect on the hot strength of steels containing them.

Alloy carbides, nitrides, and carbonitrides lead to finely dispersed precipitates which give a significant increase in the hot strength of steels (in addition to the effect of solid solution hardening). Kinetics of solution and precipitation in austenites are strongly temperature, time and deformation dependent, thus their effect on strength of a particular steel depends greatly on its thermomechanical history. The HC SS316 tested has the composition given in table (1).

Precipitation also controls the kinetics of recrystallization of austenite and can lead to indirect strength increases due to retardation of static and dynamic recrystallisation.

The following major cts can be drawn from the effects of composition e strength of hot strength of HC SS316.

(1) Very fine Nb (C, N) particles formed in strained austenite can inhibit static recrystallisation. This effect is much stronger for small deformations (e.g. 5% - 15% reduction in hot rolling).

(2) For varying strain rates and temperatures, both Nb and V have a similar effect of increasing the strength of the steel by solute and precipitation strengthening.

(3) Both V and Nb can inhibit dynamic recrystallisation. The effect of V is greater than that of Nb at lower temperature (Sage, 1979).

(4) A steel containing V and Nb would therefore be expected to exhibit a pronounced resistance to both dynamic and static recrystallisation.

(5) Precipitation plus solute hardening effects on strength are higher for a higher reheating temperature for a strain rate of (10^{-1} - 10^{-3}) s^{-1} during hot rolling.

CHOICE AND EFFECT OF THE MEAN ROLLING TEMPERATURE ($\bar{T}m$)

As a result of the chilling effect at the surface during hot rolling the Zener Hollomon parameter varies considerably with depth of stock (Sellars, 1981). The

flow stress (and the rolling load) depends on the mean temperature so it is necessary to define a suitable mean temperature for a rolling pass.

According to Harding (1976), the simplest mean which gives a correct average heat content during the pass is

$$\bar{T}_m = \frac{1}{\varepsilon_p}\int_0^{\varepsilon_p} T\, d\varepsilon \qquad (7)$$

$$\text{or } \bar{T}_m = \tfrac{1}{2}(\bar{T}_1 + \bar{T}_2) \qquad (8)$$

where εp - total equivalent strain during the pass

$\bar{T}_m$ - mean entry temperature to roll gap (°C)

$\bar{T}_2$ - mean exit temperature from roll gap (°C)

This mean temperature is the volumetric average temperature in the cross-section of the specimen.

At high strain rate ($\dot{\bar{\varepsilon}} = 1.18\ s^{-1}$) an extremely high temperature gradient is produced in the specimen near the surface w as for low strain rate ($\varepsilon = 0.08\ s^{-1}$) the extreme hig temperature gradient penetrates deep into the thick ess thus giving a huge mean temperature drop.

During roll contact, the temperature gradient through the thickness shov s a big drop of over 200°C for the low strain rate ($\dot{\bar{\varepsilon}} = 0.08\ s^{-1}$) compared to a drop of about 30°C for the high strain rate rolling ($\dot{\bar{\varepsilon}} = 1.18\ s^{-1}$) which agree with results obtained by Yanagi (1976) for rolling of SS304 on a hot strip mill roughing stand. See figure 3.

Roll chilling (or Reverse sandwich) effect caused by the cooling effect on the specimen, cold temperature of the rolls, and the speed of rolling has a significant effect on the yield stress of the specimen. This drastic temperature gradient across thickness and the drop in the mean rolling temperature are much pronounced at low strain rates.

A situation with a higher surface strength compared to a lower middle (mean) strength is created because of the temperature variation during rolling and this is what is being referred to as rell chilling (or reverse sandwich) effect. Sparling (1983) mentioned it and Barbosa (1983) referred to it as the temperature gradient effect.

Aiyedun (1984) has suggested a possible way of calculating the excess load by weighting in terms of the higher strength surface material for hot flat rolling at low strain rates.

Using the hot torsion tests on HC SS316 over the temperature range of 600°C - 1200°C and at strain rates from 3.6×10^{-3} to $1.4\ s^{-1}$, stress-strain curves were obtained given in figures (4a) to (4d). Comparison of these curves show that stress levels are increased by increasing strain rate and also by decreasing test temperatures. At low strains, work hardening causes a rapid rise in stress to a peak value σp. Recovery is the sole restoration process.

$$\text{From } \dot{\varepsilon} = A_{exp}\, Q/_{RT} \text{ for constant} \qquad (9)$$

$$\log_e \dot{\varepsilon} = \log_e A + \frac{Q}{R}\left(\frac{(1)}{T}\right) \qquad (10)$$

Strain rates for constant values of σ were plotted on a logarithmic scale against the reciprocal of the absolute temperature of deformation.

$$R \log_e\left(\frac{\dot{\varepsilon}_1}{\dot{\varepsilon}_2}\right) = Q\left(\frac{1}{T_2} - \frac{1}{T_1}\right) \qquad (11)$$

Value of Q_{def} was obtained from slope of each line from equation (11) giving a mean Q_{def} of 460 kJ/Mol. which was used to calculate the value of Z and the Z values are related uniquely to the stress.

RESULTS

Analysihg σ - ε curves from torsion tests gave figures (5a) and (5b) which show the dependence of the stress at certain value of strain on the Zener-Hollomon parameter for a constant value of the original grain size.

Two sets of equations were found to describe the stress -$\log_{10} Z$ relation.

At $Z > 1 \times 10^{17}$ (i.e. $\sigma \geq 100 Nmm^{-2}$)

$$\sigma_p = -677.3 + 45.5 \log_{10} Z \qquad (12)$$

$$\sigma_{0.1} = -482.7 + 33.7 \log_{10} Z \qquad (13)$$

$$\sigma_{ss} = -7.40.0 + 48.3 \log_{10} Z \qquad (14)$$

At $Z < 1 \times 10^{17}$ (i.e. $\sigma < 100\ Nmm^{-2}$)

$$\sigma_p = -290.6 + 22.9 \log_{10} Z \qquad (15)$$

$$\sigma_{0.1} = -252.0 + 20.0 \log_{10} Z \qquad (16)$$

$$\sigma_{ss} = -252.0 + 20.0 \log_{10} Z \quad (17)$$

At all values of Z

$$\sigma_0 = \sigma_{0.02} = -205.8 + 15.9 \log_{10} Z \quad (18)$$

$$\varepsilon_p = 0.0645 \quad Z \quad 0.039 \quad (19)$$

Data set obtained for each strain level was fitted by a straight line using the least square method to obtain equations (12) to (19).

Strain to peak stress (ε_p) is generally related to the Zener Hollomon parameter by the equation

$$\varepsilon_p \propto d_o^{\,n} Z^m \quad (20)$$

From the relationship of ε_p to Z, m was found to be equal to ~ 0.039 giving equation (19).

Peak stress (σ_p) vs $\log_{10}$ Z and $\sigma_{0.1}$ vs $\log_{10}$ Z obtained for HC SS316 using hot torsion test were compared with results obtained by various researchers for a similar SS316 using different modes of hot deformation in figures (a) and (6b).

ESTIMATION OF YIELD STRESS ACROSS THICKNESS

From plots of strain rate ($\dot{\varepsilon}$) and Temperature (T) against strain; plot of Zener Hollomon parameter (Z) against strain and stress-strain (σ - ε) curves for variable Z for specimen rolled at low strain rate ($\dot{\varepsilon}$ ~ 0.08 - 1.5 s^{-1}) and low reductions (r ~10%) as given in figures 1 and 2, the yield stress across the material thickness was estimated as follows:

(i) Based on data from tables (2) - (6), a half thickness profile was subdivided into 3 zones (a, b and c), each 1/3 of the half thickness. The temperature profile in the half thickness as a whole as well as in each of zones a, b and c were also obtained during the roll contact.

Knowing ε_m, ε_n and ε_n, A_i and $\dot{\varepsilon}_m$ values were obtained from equations 21 and 22.

ε_m - maximum strain on σ-ε curve

ε_n - " " " " " " for $^1/_2$ profile analysis

ε_n - " " rate " " for $^1/_2$ profile analysis

$$A_i = \varepsilon_m / \varepsilon_n \quad (21)$$

$$\text{and } \dot{\varepsilon}_m = \dot{\varepsilon}_n \times A_i \quad (22)$$

Finding T_{av} for each third (a, b and c) for different t values, thus

$T_{i's}$ were obtained where

t_i = Instanteneous time during roll contact

T_i = " Temperature during roll contact

Z_i = " Zener Hollomon's Parameter (Z) during roll contact

See figure 7a and 7b.

(ii) Using $\dot{\varepsilon}_m$ and $T_{i's}$ (^{0}K), values of Z_i were obtained using equation (6)

(iii) Using Z_i values, σ_0, $\sigma_{0.1}$ ε_p, σ_p, and σ_{ss} were obtained from equations (12) - (19).

(iv) σ-ε curves were then plotted for different Z_i values for

(a) whole half profile

(b) Portions (a), (b), and (c)

all on the same graph. See figure (8)

(v) Defining $\bar{\sigma}_G = \frac{1}{\varepsilon_m} \left(\frac{W}{V}\right) = \frac{1}{\varepsilon_m} \int_o^{\varepsilon_m} \sigma d\varepsilon$

where (W. D/V) is work done per unit volume

$$\frac{1}{\varepsilon_m} \int_o^{\varepsilon_m} \sigma d\varepsilon = \frac{[\sigma_1 + \sigma (\varepsilon_1 + \varepsilon_2) + \frac{\sigma_2 + \sigma_3}{2}}{2}$$

$$(\varepsilon_3 - \varepsilon_2) + ... + \frac{(\sigma_{n-1} + \sigma_n)}{2} (\varepsilon_n - \varepsilon_{n-1})] \quad (23)$$

$$\bar{\sigma}_g = {}^1/_3 (\bar{\sigma}_{ga} + \bar{\sigma}_{gb} + \bar{\sigma}_{gc}) \quad (24)$$

$$\bar{\sigma}_{g^*} = \frac{1}{\varepsilon_m} [{}^1/_3 (\bar{\sigma}_{ga} \cdot \varepsilon_a + \bar{\sigma}_{gb} \cdot \varepsilon_b + \bar{\sigma}_{gc} \cdot \varepsilon_c)] \quad (25)$$

(vi) Using equation (23) and (24), $\bar{\sigma}_{ga}$, $\bar{\sigma}_{gb}$ $\bar{\sigma}_{gc}$ and $\bar{\sigma}_g$ were obtained from (iv) (b) above.

(vii) Using equation (25) $\bar{\sigma}_g$* was obtained.

Based on the foregoing, it was then possible to compare $\bar{\sigma}_{ga}$: $\bar{\sigma}_{gb}$: $\bar{\sigma}_{gc}$: and also to compare $\bar{\sigma}^*_g$: $\bar{\sigma}_g$: $\bar{\sigma}_G$:

Results of the yield stress variation across thickness for this material HC SS316 specimen hot rolled at low reduction (~10%) and at low strain rate ($\dot{\varepsilon}$ ~0.08 s^{-1}) are given in table 7.

The surface $^1/_3$ element of the half thickness (Zone a) has a strain increase of ~15%, with a corresponding increase of ~1 x 10^4 (3.5 x 10^{20} - 3.5 x 10^{24}) in the Z value and a decrease of ~250°C in the mean rolling temperate ($\bar{T}_m$).

These corresponded to an increase of~200 N_{mm}^{-2} (100 to 300) in the mean yield stress ($\bar{\sigma}_a$) of zone a and the $\bar{\sigma}_g^*$ (YKP & YKG) value of the complete specimen increased by ~35%. The ratio of $\bar{\sigma}_{ga}$ $\bar{\sigma}_{gb}$: $\bar{\sigma}_{gc}$ = 2.8: 1.3: 1.0 i. e. Ratio of mean yield stress of the 3 zones, a, b, c, and $\bar{\sigma}_g^*$: $\bar{\sigma}_g$: $\bar{\sigma}_G$ 1.36: 1.01: 1.0

DISCUSSION

The general shape of the σ-ε curves obtained from HC SS316 samples tested in hot torsion (isothermally) Fig. 4a - 4d shows the following characteristics:

(a) A steep work hardening zone followed by,

(b) a shallow and wide minimum stress region and/or

(c) a gentle transition into the steady state part of the curve.

The set of equations (12) - (19) used to describe the stress-strain curves imply the applicability of the power law ($\dot{\varepsilon} = A\sigma^n$) at low stresses (< 100 N_{mm-2}) and an exponential law [$\dot{\varepsilon} = A' \exp(\beta\sigma)$] at high stresses (> 100 N_{mm-2}) as obtained by Cole (1979) for 18/8 stainless steel (austenitic). The value of ε_p obtained in equation (19) is in reasonable agreement with ε_p = 0.097 Z 0.032 obtained by Barbosa (1983) for SS316L.

The ratio of $\bar{\sigma}_g^*$ $\bar{\sigma}_g$: $\bar{\sigma}_G$ obtained provided a way of weighting in terms of the surface temperature for hot rolling at low strain rates. It takes into account the strain variation from centre to surface and the temperature variation from centre to surface during the roll contact.

The values of YKP and YKG (i.e. k_p and k_g mean yield strength for load and torque calculations respectively) being used previously for the calculation of Total Load and Torque by Sim's Method or by Bland and Ford's Mehod were less than $\bar{\sigma}_G$ calculated above. This then explains why calculated values of Load and Torque (By Sim's or B & F) were much lower than experimental Rolling Loads and Torques.

The ratio of $\bar{\sigma}_{ga}$ $\bar{\sigma}_{gb}$: $\bar{\sigma}_{gc}$ obtained confirm the reverse sandwich (or roll chilling) effect for the hot rolling at low strain rates, giving an almost 3 times increase in the yield strength of the surface material compare to the centre material.

The $\bar{\sigma}_{gb}^*$ given in equation (25) provide a good method of estimating the mean yield strength of the material being hot rolled at low strain rate. It combines the temperature and strain effect as well as the composition effect.

$$\frac{\bar{\sigma}_s}{\bar{\sigma}_m} = n \qquad (26)$$

This n value has been used effectively in estimating the chilling effect correction factor (c. e. f.) which has been in correcting rolling loads and torques by Sim's method or Bland and Ford's Method. Aiyedun (1984)

CONCLUSIONS

From this work, the following conclusions can be drawn:

1. At high strain rates (> 1.5 s^{-1}) for hot flat rolling a steep temperature gradient is produced in the specimen near the surface whereas for low strain rates (0.80 -1.5 s^{-1}), this temperature gradient penetrates deep into the thickness leading to a large drop in mean temperature during a rolling pass.

2. The use of the mean entry temperature to the roll gap as the appropriate temperature for calculating rolling loads and torques (which is satisfactory for high strain rates $\dot{\bar{\varepsilon}} \geq 5.0\ s^{-1}$ lead to serious underestimates of the actual measured loads and torques at low strain rates ($\dot{\bar{\varepsilon}}$ = 0.08 - 1.5 s^{-1})

3. The drastic temperature gradient across thickness and the big drop in the mean rolling temperature for hot rolling at low strain rates lead to what is called "roll chilling effect". This effect is analogous to rolling or compressing a composite material with hard surface strips and a soft central strips and can therefore be considered as a "reverse sandwich" effect.

4. The yield strength of HC SS316 was obtained from the hot torsion tests and expressed as equations using the following: peak stress (σ_p) stress to 0.1 strain ($\sigma_{0.1}$) steady state stress (σ_{ss}), stress to 0.02 strain (σ_o) and peak strain (ε_p)in terms of the Zener Hollomon parameter, (Z); see equation (12) - (19). The stress-strain (σ–ε) equations for any value of Z was then obtained using these derived equations.

5. For varying strain rates and temperatures, both Nb and V present in HC SS316 have similar and additive effect of increasing the strength of the steel by solute and precipitation strengthening. These were higher for a higher reheating temperature for strain rate 10^{-1} to 10^{-3} s^{-1} during hot rolling.

6. For accurate rolling load and torque, the correct mean yield stress or stress-strain curve must be used.

7. A 35% increase in the mean yield stress (σ_g *) obtained was due to:

(a) A temperature effect leading to a temperature (and flow stress) gradient and a drastic drop in the mean rolling temperature set up by the roll chilling effect and

(b) The formation of fine precipitates of Nb (C, N) and V (C, N) produced by the material composition and the rolling conditions. This increase with straining and a longer time of contact making it more pronounced at lower strain rates.

ACKNOWLEDGEMENT

The author wishes to acknowledge the assistance of Prof. C. M. Sellars, Dr. L. G. M. Sparling and Mr. Mike Hudson, all of the University of Sheffield where this work was carried out.

REFERENCES

1. **ALTAN, T. and BOULGER, F. W.** (1973) 'Flow Stress of Metals and its Application in Metal Forming Analysis". Trans. ASME, Journal of Engineering for Industry, p. 1009-1019.

2. **VENTER, R. D. and ABD-RABBO, A.** (1980) "Modelling of the Rolling Process I and II".Int. J. Mech. Sci., Vol. 22,1980 p. 83-92 and p. 93-98.

3. **SUZUKI, H. et al.** (1968) "Studies on Flow Stress of Metals and Alloys". Vol.18 (3),, Ser. No. 117, Reports by the Institute of Industrial Sciences, University of Tokyo.

4. **SPARLING, L. G. M.** (1983) "The Evaluation of Load and Torque in Hot Flat Rolling from Slipline Fields." "Proc. Instn. Mech. Engrs., Vol. 197A, p. 277-285.

5. **AIYEDUN, P. O.** (1984) Ph.D. Thesis, University of Sheffield.

6. **SELLARS, C. M. et al** (1976) "Plane Strain Compression Testing at Elevated Temperatures" Report on Research work supported by SRC Grant No. B/R6/1481.

7 **BARRACLOUGH, D. R.** (1974) Ph.D. Thesis, Sheffield Universi

8. **SAH, J. P.** (1970) h.D Thesis, Sheffield University.

9. **COLE, A. T.** (1979) Ph.D. Thesis, Sheffield University.

10. **ROBERTS, W. L.** (1978) "Cold Rolling of Steel" Marcel Dekker Inc. Publishers, New York.

11. **ZENER, C. and HOLLOMON, J. H.** (1944) "Effect of Strain Rate upon Plastic Flow of Steel". J. Appl. Physics, Vol. 15, p. 22 - 32.

12 **TEGART, W. J. McG. AND GITTINS, A.** (1976) "The Hot Deformation of Austenite". Ed. J.B. Balance.

13. **SAGE, A. M.** (1979) "Developments in Control Rolling of Vanadium Bearing Steels". Hot Working and Forming Processes, Ed. C.M Sellars and G.J. Davies, Metals Soc. Confr., Sheffield.

14. **SELLARS, C. M.**(1981) "Les Traitments Thermomecaniques" 24eme Colloque de Metallurgie, Institut National des Sciences et Technique Nucleaires, Sanclay, p.111-120

15. **HARDING, R. A.** (1976) Ph.D. Thesis, Sheffield University.

16. **YANAGI, K** (1976) Trans I.S.I.J., Vol.16, p.11

17. **BARBOSA, R. A. N. M.** (1983) Ph.D. Thesis, Sheffield University.

TABLE AND FIGURE CAPTIONS

Table (1) - Chemical Composition of Steels Used.

Table (2) - Strain, Strain Rate, Temperature, Peak Strain and Z values for SP, PN1 -$^1/_2$ Profile.

Table (3) - Time, Strain, Temperature for (a), (b) and (c) of SP. PN1 during roll contact.

Table (4) - Strain, Strain Rate, Temperature, Peak Strain and Z values for SP, PN1 (a-zone)

Table (5) - Strain, Strain Rate, Temperature, Peak Strain and Z values for SP, PN1 (b-zone).

Table (6) - Strain, Strain Rate, Temperature, Peak Strain and Z values for SP, PN1 (c-zone).

Table (7) - Yield Stress variation across thickness for HC SS316 specimen hot rolled at low reduction (r ~10%) and low strain rate ($\dot{\varepsilon}$~0.08 s-1)

Table (8) - List of Symbols

Fig. (1) - Plot of $\dot{\varepsilon}$ vs ε and T vs ε for SP.PN1 hot rolled at low reduction (r~ 10%) and low strain rate (ε~0.08 s^{-1})

Fig. (2a) - Z vs ε for variable Z for SP.PN1 rolled at low strain rate and low reduction.

Fig. 2b - Plot of σ-ε curve for variable Z and for Z for SP.PN1 rolled at low strain rate and low reduction.

Fig. 3 - Temperature across thickness for HC SS316 hot roll at slow and fast strain rates on mill A at different times during and after roll contact (T_f~1125°C, r ~10%)

Fig. 4 - Stress-strain curves for HC SS316 samples tested in torsion at various temperatures and strain rates:

4a - $\dot{\bar{\varepsilon}}$ = 0.0036 s^{-1}, T = 600 - 1200°C

4b - $\dot{\bar{\varepsilon}}$ = 0.0289 s^{-1}, T = 600 - 1200°C

4c - $\dot{\bar{\varepsilon}}$ = 0.359 s^{-1}, T = 800 - 1100°C

4d - $\dot{\bar{\varepsilon}}$ = 1.3989 s^{-1}, T = 800 - 1200°C

Fig. 5a - Dependence of the peak stress on Zener-Hollomon parameter (Z) for HC SS316 using torsion tests.

Fig. 5b - Dependence of the stress at 0.1 strain on Zener-Hollomon parameter for HC SS316

Fig. 6a - Peak stress (σ_p) vs $\log_{(10)}Z$ for this work compared to results on SS316 by other researchers under different kinds of tests.

Fig. 6b - Stress to 0.1 strain ($\sigma_{0.1}$) vs $\log_{(10)}Z$ for this work compared to results on SS316 obtained by other researchers under different kinds of tests.

Fig. 7a - Strain profile across zone a, b, c, of Thickness

Fig. 7b - Temperature profile in zone a, b, c, during roll contact.

Fig. 8 - Stress-strain (σ.ε_m) curve for zones a, b, and c, and for complete $^1/_2$ profile of SP.PN1 during roll contact.

TABLE 1: CHEMICAL COMPOSITION OF STEELS USED

Elements	Wrought HC SS316 (As-Received)	HC SS316		Method
C	% wt	% wt	± Acc.	Leco
C	0.051	0.054	0.001	Leco
S	0.017	0.016	0.003	Leco
Mo	2.12	2.05	0.02	Quantometer
Ni	11.22	11.3	0.2	Quantometer
Si	0.53	0.54	0.02	Quantometer
Cr	17.20	17.4	0.2	Quantometer
W		<0.02	-	Quantometer
Mn	1.34	1.37	0.02	Quantometer
Nb		0.10	0.02	Quantometer
V		0.07	0.02	Quantometer
Ti		0.04	0.02	Quantometer
Co		0.14	0.02	Quantometer
Cu		0.32	0.02	Quantometer
N		524ppm	10ppm	Leco
O		122ppm	10ppm	Leco
P	0.024			Quantometer
Fe				Quantometer
Mg				Quantometer
Zn				Quantometer
Al				Quantometer

*WROUGHT HC SS316 was from heat 38256-2C.

Mean Grain Size (um) = 39.3 ± 2.3

TABLE 2: STRAIN, STRAIN RATE, TEMPERATURE, PEAK STRAIN AND Z VALUES FOR SP. PN1 - $^1/_2$ PROFILE

Strain εm	Strain Rate $\dot{\varepsilon} m$	Temperature ^0K	Peak Strain εp	Zener-Hollomon Parameter Z
0.0	0.188	1286	0.37	9.3109×10^{17}
0.005	0.186	1240.1	0.38	4.5270×10^{18}
0.015	0.182	1226.9	0.39	7.1488×10^{18}
0.033	0.173	1203.0	0.40	1.1668×10^{19}
0.068	0.155	1168.8	0.42	5.7194×10^{19}
0.124	0.114	1119.6	0.44	3.3673×10^{20}
0.181	0.021	1047.2	0.47	1.9193×10^{21}
0.183	0.0	1033.7	0.37	1.8056×10^{18}

TABLE 3: TIME, STRAIN, TEMPERATURE FOR (a), (b) and (c) of SP. PNI DURING ROLL CONTACT

Time t (s)	Strain εm	TEMPERATURE (a) Zone Ti (a)^{0}C	(b) Zone Ti (b)^{0}C	(c) Zone Ti (c)^{0}C
0.0	0.0	1006.4	1014.3	1018.3
0.023	0.004	868.8	1014.2	1018.2
0.068	0.011	831.2	1014.2	1018.1
0.159	0.024	766.3	1005.8	1018.0
0.341	0.050	701.3	970.1	1016.1
0.704	0.091	644.9	899.5	995.4
1.431	0.133	599.7	805.9	916.9
1.590	0.134	593.1	790.3	899.7

TABLE 4: STRAIN, STRAIN RATE, TEMPERATURE, PEAK STRAIN AND Z VALUES FOR SP. PN1 (a-Zone)

Strain εm	Strain Rate εm	Temperature ^0K	Peak Strain εp	Zener-Hollomon Parameter Z
0.0	0.159	1279.4	0.36	9.8031×10^{17}
0.004	0.157	1141.8	0.43	1.7794×10^{20}
0.012	0.153	1104.3	0.45	9.0429×10^{20}
0.028	0.146	1039.3	0.50	1.9781×10^{22}
0.057	0.130	974.3	0.56	6.1714×10^{23}
0.105	0.096	917.9	0.62	1.4799×10^{25}
0.153	0.018	872.7	0.65	6.2830×10^{25}
0.155	0.0	866.1	0.52	5.7153×10^{22}

TABLE 5: STRAIN, STRAIN RATE, TEMPERATURE, PEAK STRAIN AND Z VALUES FOR SP. PN1 (b-Zone)

Strain εm	Strain Rate εm	Temperature ^0K	Peak Strain εp	Zener-Hollomon Parameter Z
0.0	0.140	1287.3	0.36	6.6432×10^{17}
0.004	0.139	1287.2	0.36	6.5759×10^{17}
0.011	0.136	1287.2	0.36	6.4396×10^{17}
0.025	0.129	1278.8	0.36	8.1292×10^{17}
0.050	0.115	1243.1	0.38	2.5086×10^{18}
0.094	0.085	1172.5	0.41	2.6993×10^{19}
0.135	0.016	1078.9	0.44	3.0251×10^{20}
0.137	0.0	1063.3	0.36	4.0763×10^{17}

TABLE 6: STRAIN, STRAIN RATE, TEMPERATURE, PEAK STRAIN AND Z VALUES FOR SP. PN1 (c-Zone)

Strain εm	Strain Rate $\dot{\varepsilon} m$	Temperature ^0K	Peak Strain εp	Zener-Hollomon Parameter Z
0.0	0.139	1291.3	0.36	5.7688×10^{17}
0.004	0.138	1291.2	0.36	5.7157×10^{17}
0.011	0.134	1291.1	0.36	5.5962×10^{17}
0.025	0.128	1291.0	0.36	5.3503×10^{17}
0.050	0.114	1289.1	0.36	5.0912×10^{17}
0.092	0.084	1268.4	0.36	7.5476×10^{17}
0.134	0.016	1189.9	0.38	2.4896×10^{18}
0.135	0.0	1171.7	0.30	3.2950×10^{15}

TABLE 7: YIELD STRESS VARIATION ACROSS THICKNESS FOR HC SS316 SPECIMEN HOT ROLLED AT LOW REDUCTION (~10%) AND LOW STRAIN RATE ($\dot{\varepsilon} \sim 0.08\ s^{-1}$)

$\overline{\sigma}_{ga}$	=	336.95	$N_{mm^{-2}}$
$\overline{\sigma}_{gb}$	=	157.05	"
$\overline{\sigma}_{gc}$	=	121.26	"
$\overline{\sigma}_{g}$	=	205.09	"
$\overline{\sigma}_{G}$	=	203.10	"
$\overline{\sigma}_{g}^{*}$	=	276.58	"
$\overline{\sigma}_{ga}$: $\overline{\sigma}_{gb}$: $\overline{\sigma}_{gc}$	=	2.8: 1.3: 1.0	
$\overline{\sigma}_{g}^{*}$: $\overline{\sigma}_{g}$: $\overline{\sigma}_{G}$	=	1.36: 1.01 1.0	

TABLE 8: LIST OF SYMBOLS

$k, \bar{k}$	instanteneous yield stress; mean yield stress (N_{mm}^{-2})
$\bar{k}_p, \bar{k}_g$	mean yield strength for Load and Torque calculations (N_{mm}^{-2})
r	rolling reduction percentage
θ	angle substended by a point on roll surface at centre of curvature of arc of contact with respect to line joining roll centres.
α	angle of entry (i.e. max. value of θ)
h_1, h_2	initial and final thickness of specimen (mm)
Q	Activation Energy for deformation associated with the temperature dependence of the flow stress
R	Gas constant
T	Temperature Absolute (°K)
σ_p	Stress at peak strain
$\sigma_{0.1}$	Stress at 0.1 strain
σ_{ss}	Stress at steady state strain
σ_o	Stress at zero strain
Z	Zener-Hollomon Parameter
ε_p	Strain for peak stress
$\varepsilon_m, \dot{\varepsilon}_m$	Maximum strain, max strain rate on σ-ε curve
$\varepsilon_n, \dot{\varepsilon}_n$	Strain, strain rate on σ-ε curve for $^1/_2$ profile analysis
t_i, T_i, Z_i	Instanteneous time, temperature, Zener-Hollomon Parameter during roll contact.
$\bar{\sigma}_G$	Yield strength for whole profile defined as $\frac{1}{\varepsilon_m} \cdot \frac{(W.D)}{V} = \frac{1}{\varepsilon_m} \int_o^{\varepsilon_m} \sigma \, d\varepsilon$
$\bar{\sigma}_{ga}, \bar{\sigma}_{gb}, \bar{\sigma}_{gc}$,	Yield strength for $^1/_3$ of half profile defined as zones a, b, and c: $\left(\frac{W.D}{V}\right) a = \int_o^{\varepsilon_{mo}} \sigma d\varepsilon$
$\bar{\sigma}_g$	Yield strength for whole profile defined as = 1/3 $(\sigma_{ga} + \sigma_{gb} + \sigma_{gc})$
$\bar{\sigma}_g^*$	Yield strength for the whole profile defined as = $\frac{1}{\varepsilon_n} [1/3 \ (\bar{\sigma}_{ga} \cdot \varepsilon_a + \bar{\sigma}_{gb} \cdot \varepsilon_b + \bar{\sigma}_{gc} \cdot \varepsilon_c)]$

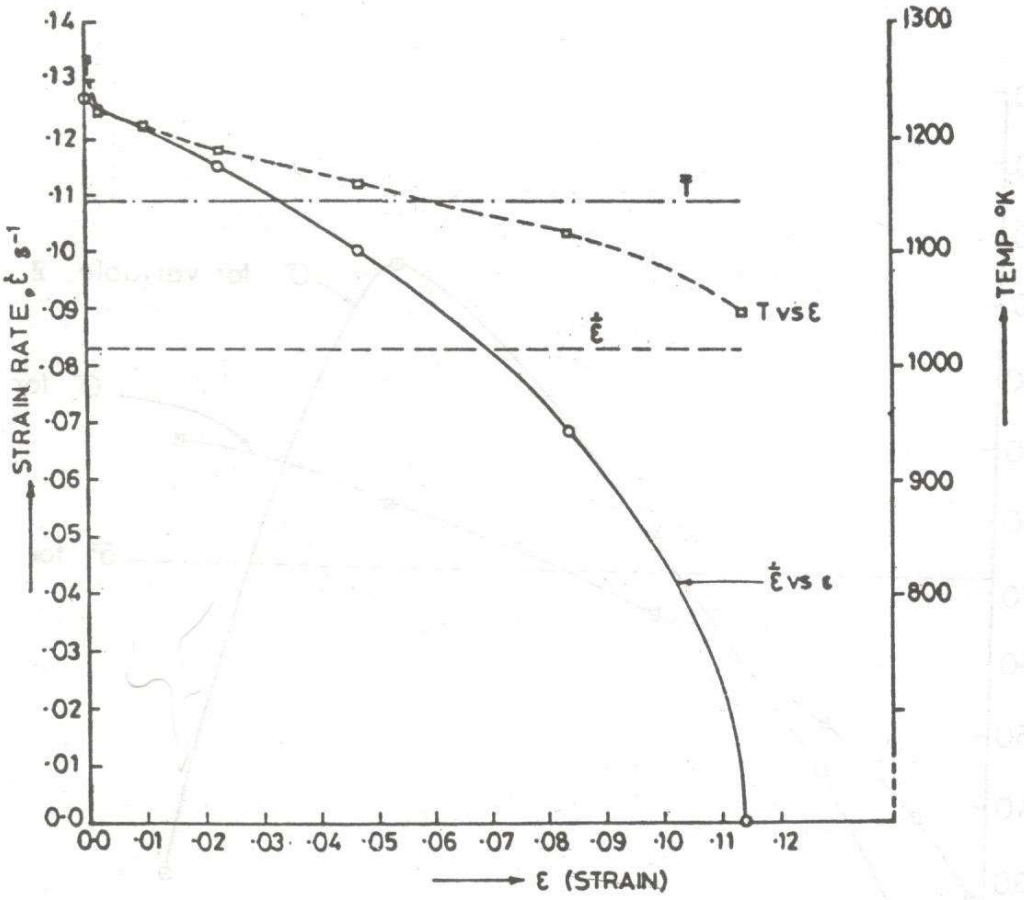


FIG. 1. PLOT of $\dot{\varepsilon}$ v ε and T vs ε for SP. PNI hot rolled at low reduction (r~10%) and low strain rate ($\dot{\bar{\varepsilon}}$ ~0·08 s^{-1})

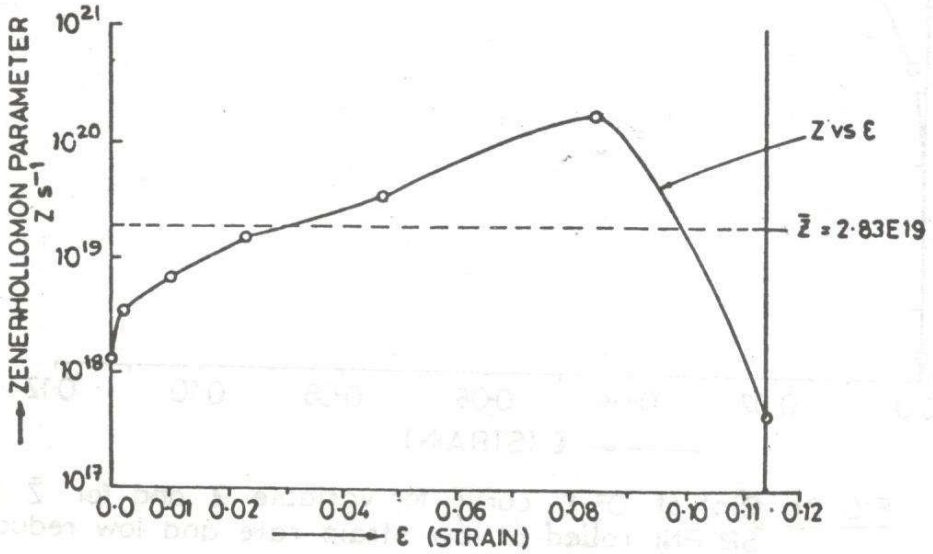


FIG. 2a. Z vs ε for variable Z for SP·PNI rolled at low strain rate and low reduction.

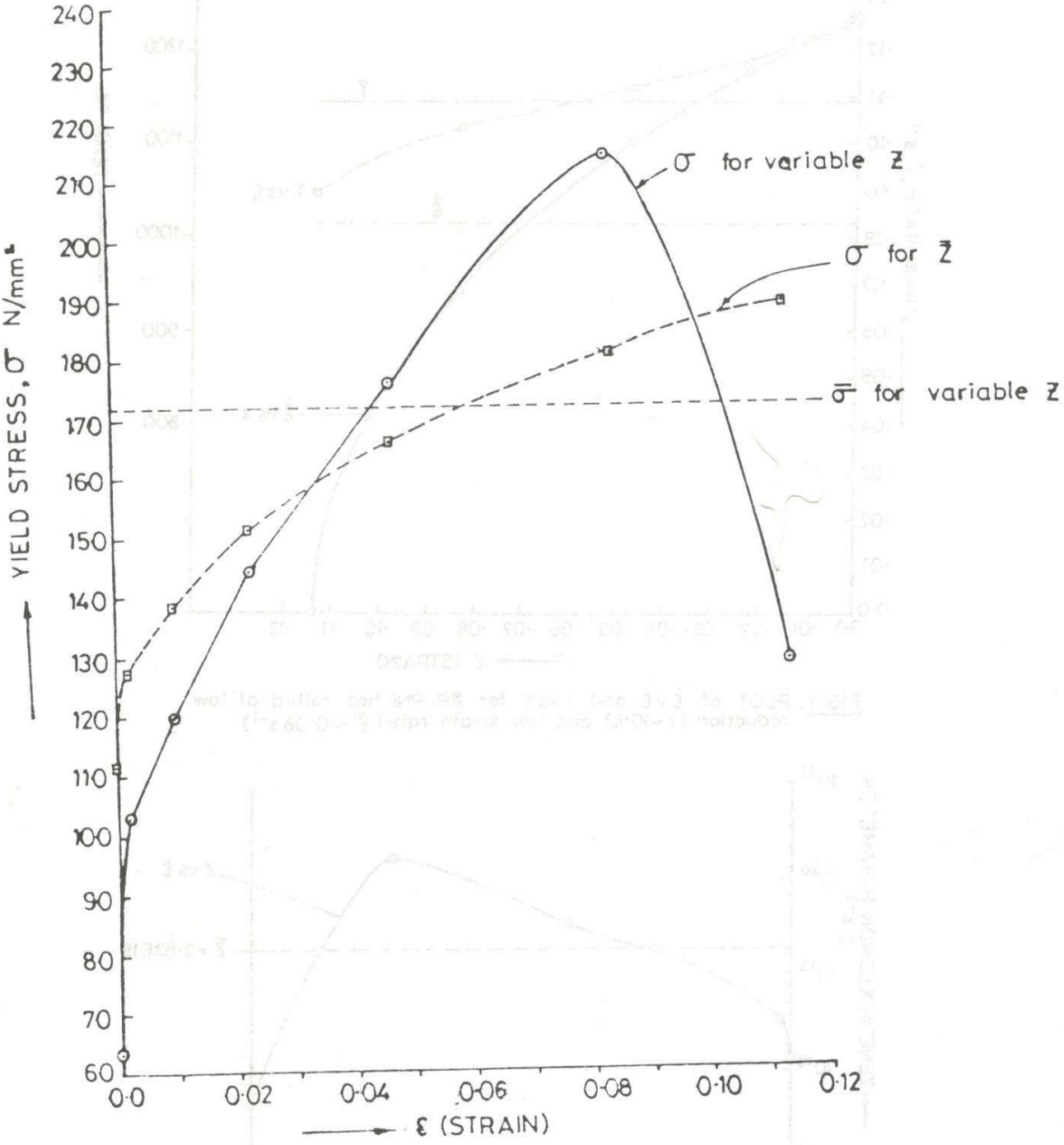


FIG. 2b. Plot of σ ε curve for variable Z and for $\bar{Z}$ for SP PNI rolled at low strain rate and low reduction.

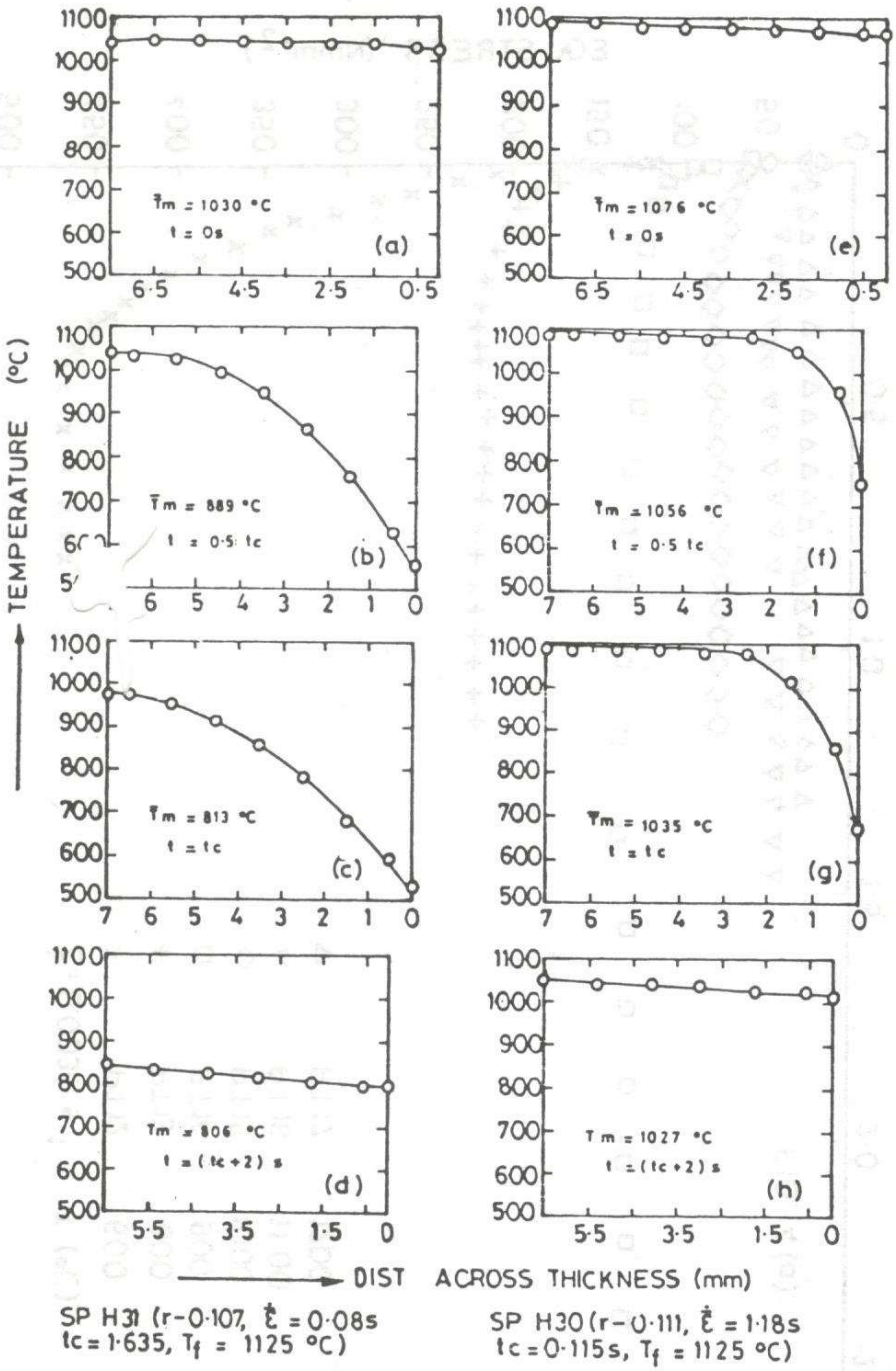


FIG. 3. Temperature across thickness for HC SS 316 hot rolled at slow and fast strain rates on mill A at different times during and after roll contact (T ~ 1125 °C, r ~ 10%).

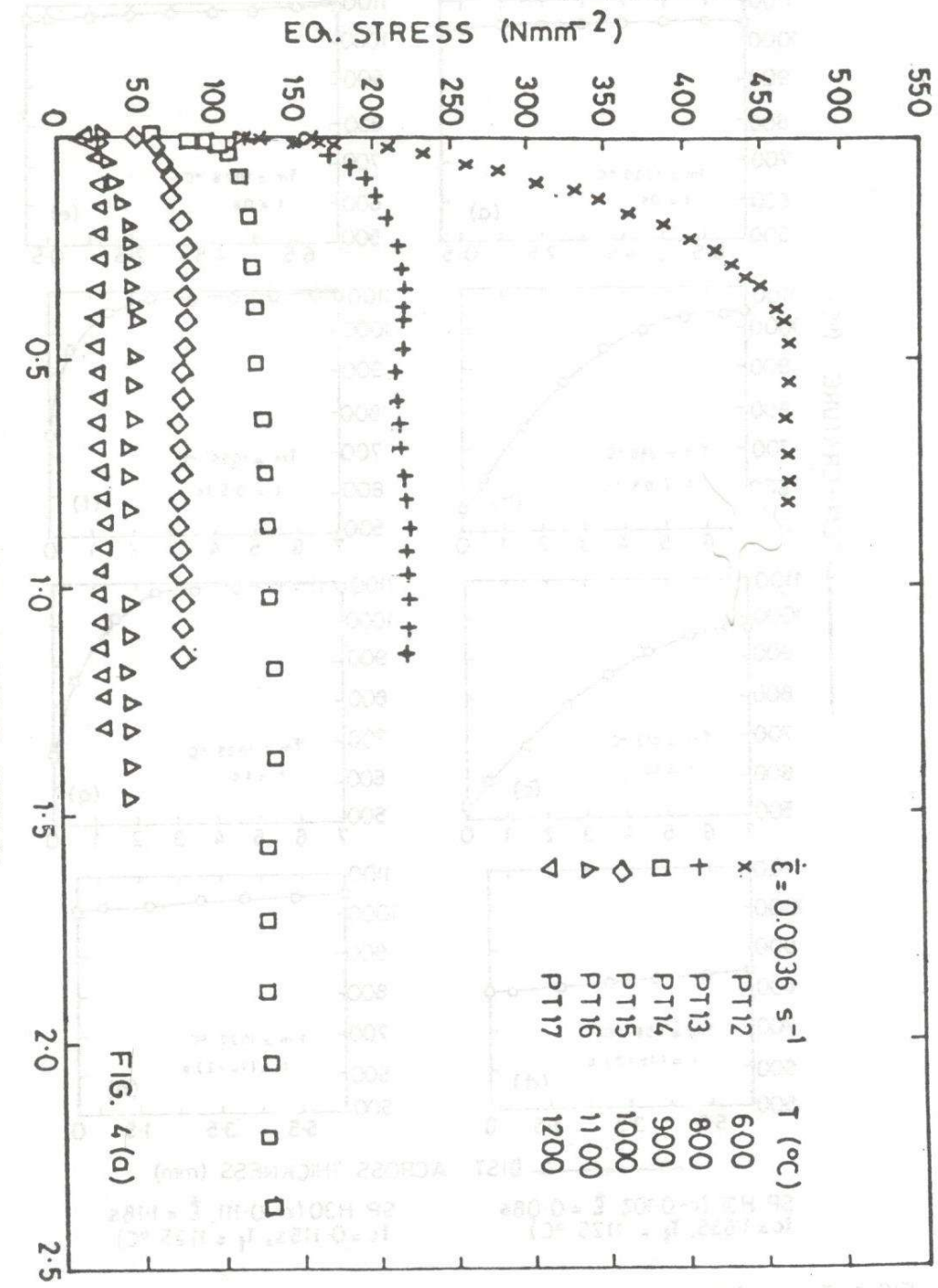


FIG. 4. Stress-strain curves for HC SS 316 samples tested in torsion at various temperatures and strain rates.

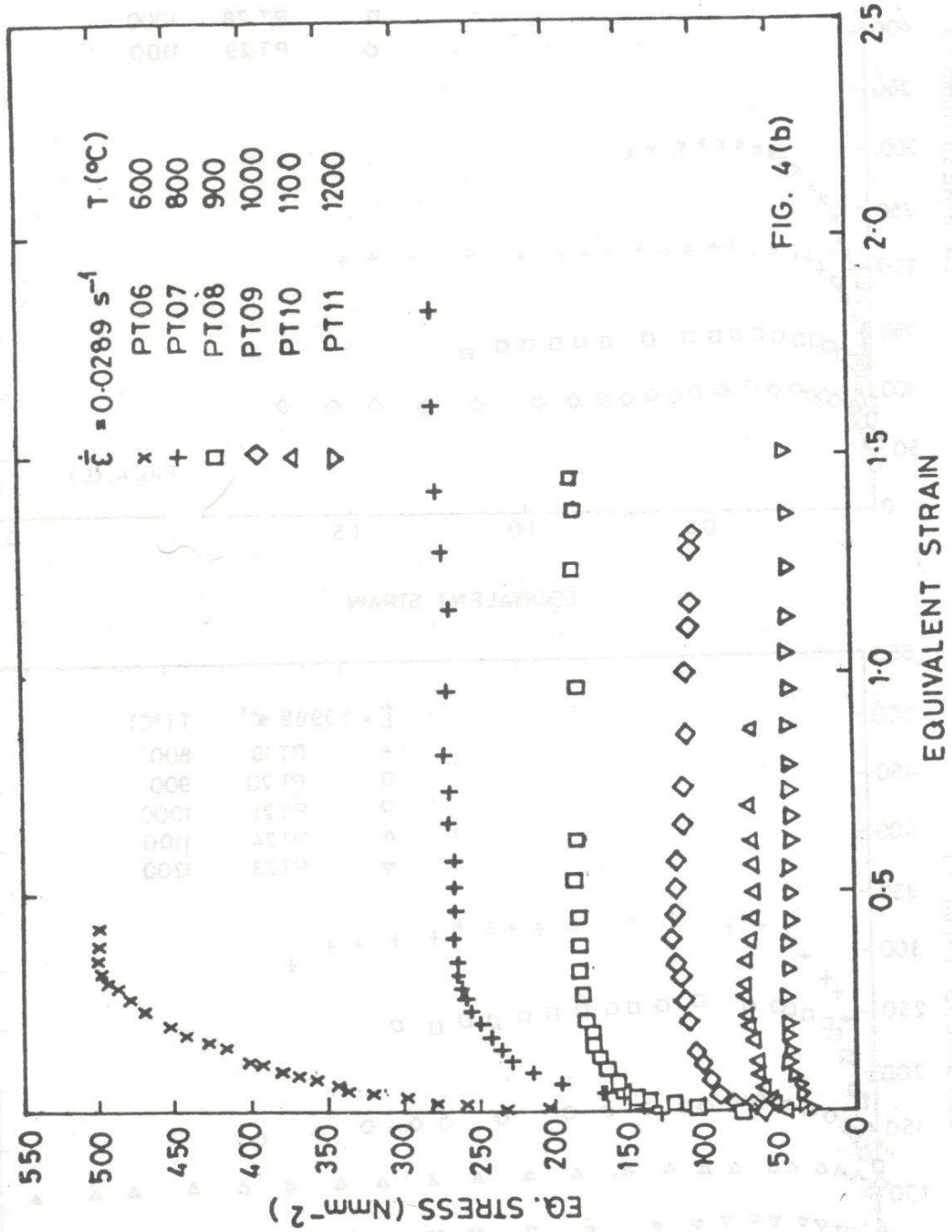

$\dot{\bar{\varepsilon}}$ =0·0289 s^{-1}
T (°C)
PT06 600
PT07 800
PT08 900
PT09 1000
PT10 1100
PT11 1200
EQ. STRESS (Nmm^{-2})
EQUIVALENT STRAIN
0
50
100
150
200
250
300
350
400
450
500
550
0·5
1·0
1·5
2·0
2·5

FIG. 4 (b)

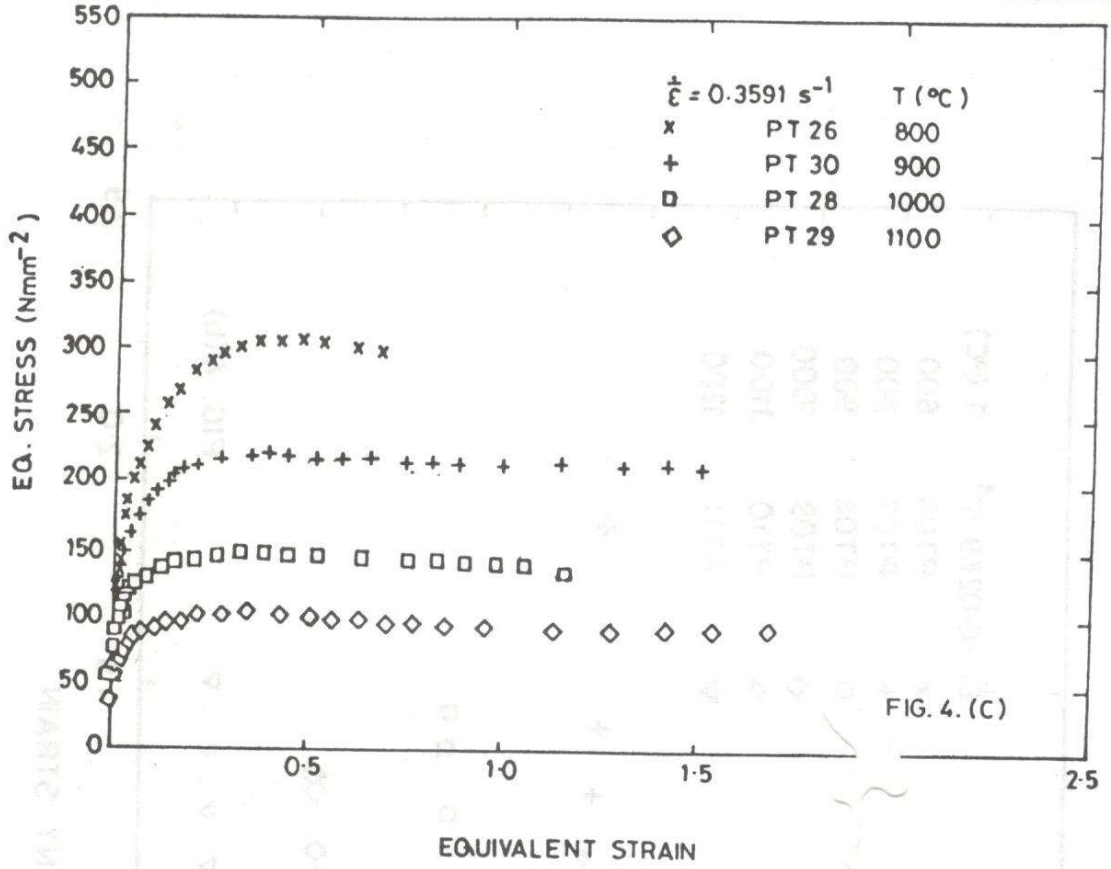

$\dot{\bar{\varepsilon}}$ = 0.3591 s^{-1} T (°C)
PT 26 800
PT 30 900
PT 28 1000
PT 29 1100
EQ. STRESS (Nmm^{-2})
EQUIVALENT STRAIN
0 50 100 150 200 250 300 350 400 450 500 550
0·5 1·0 1·5 2·5

FIG. 4. (C)

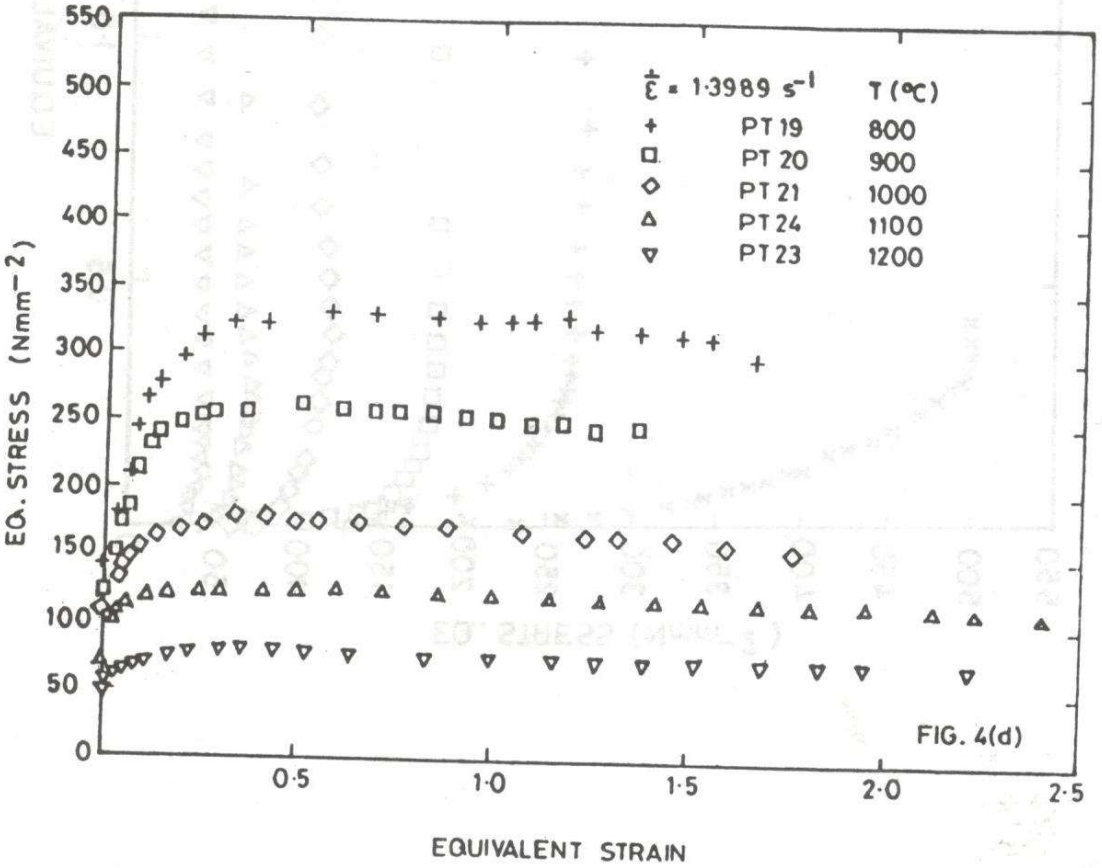

$\dot{\bar{\varepsilon}}$ = 1·3989 s^{-1} T (°C)
PT 19 800
PT 20 900
PT 21 1000
PT 24 1100
PT 23 1200
EQ. STRESS (Nmm^{-2})
EQUIVALENT STRAIN
0 50 100 150 200 250 300 350 400 450 500 550
0·5 1·0 1·5 2·0 2·5

FIG. 4(d)

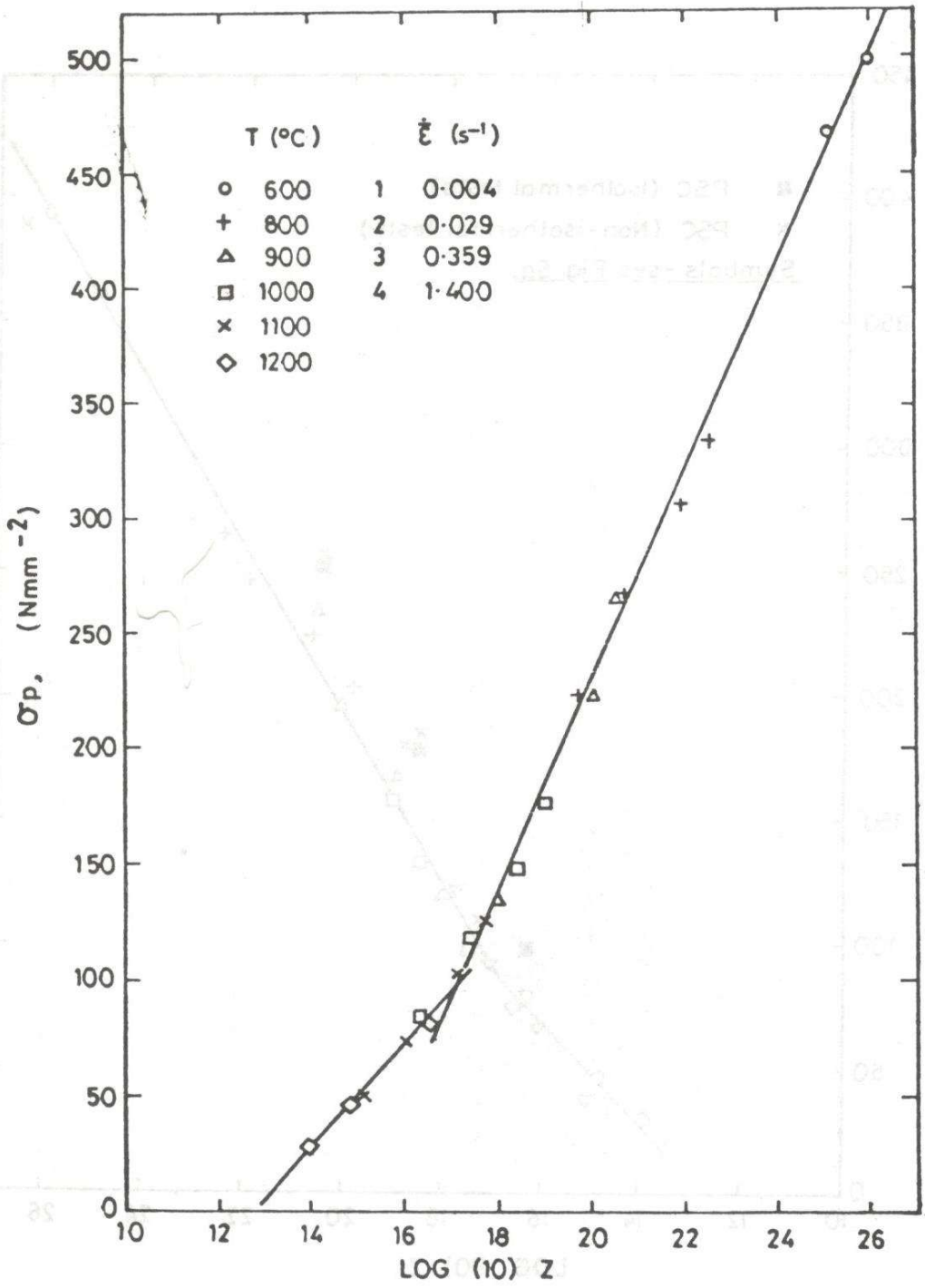


FIG. 5a. Dependence of the peak stress on Zener-Hollomon parameter for HC SS 316 using torion tests.

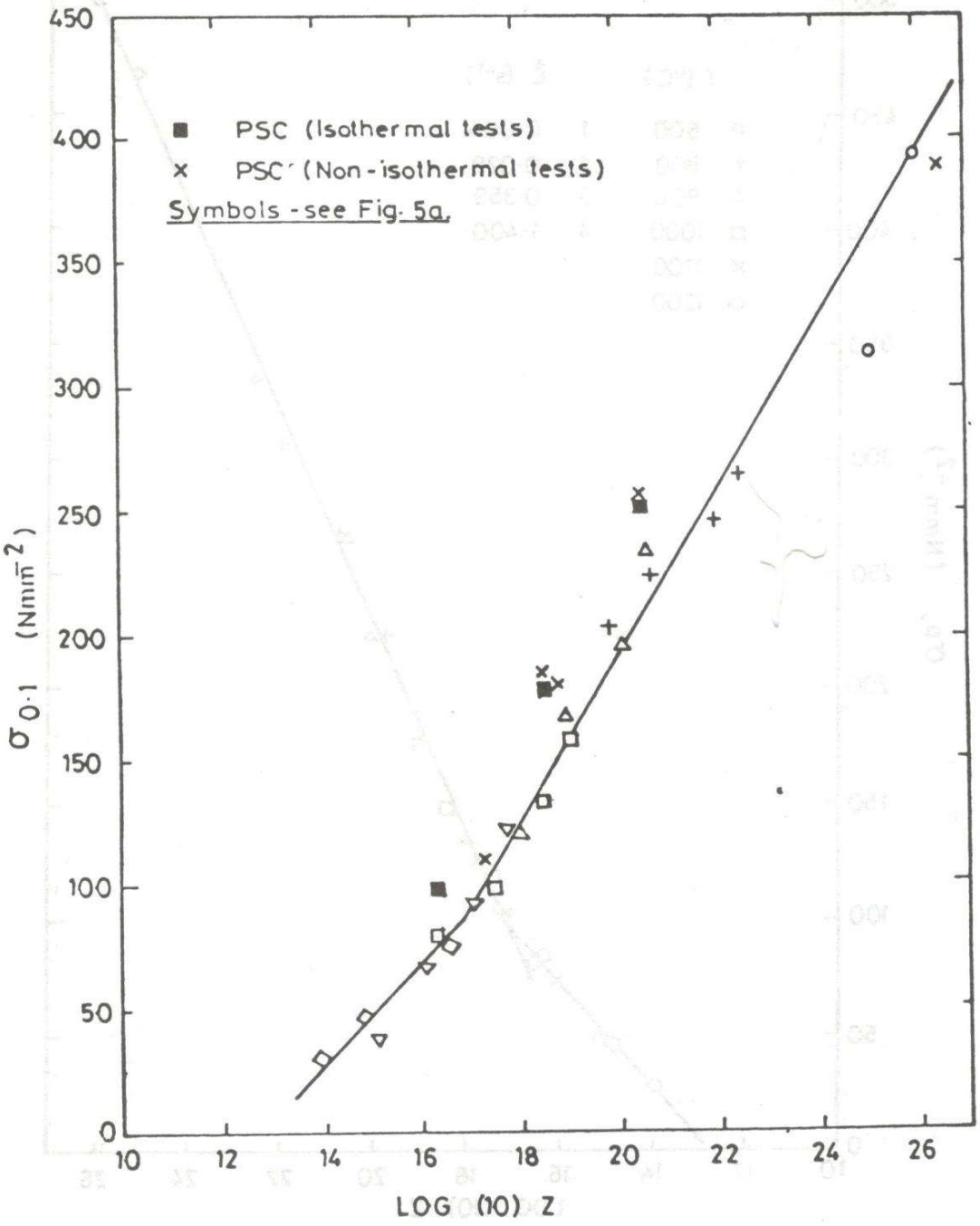


FIG. 5b. Dependence of the stress at 0·1 strain on Zener - Hollomon parameter for HC SS 316.

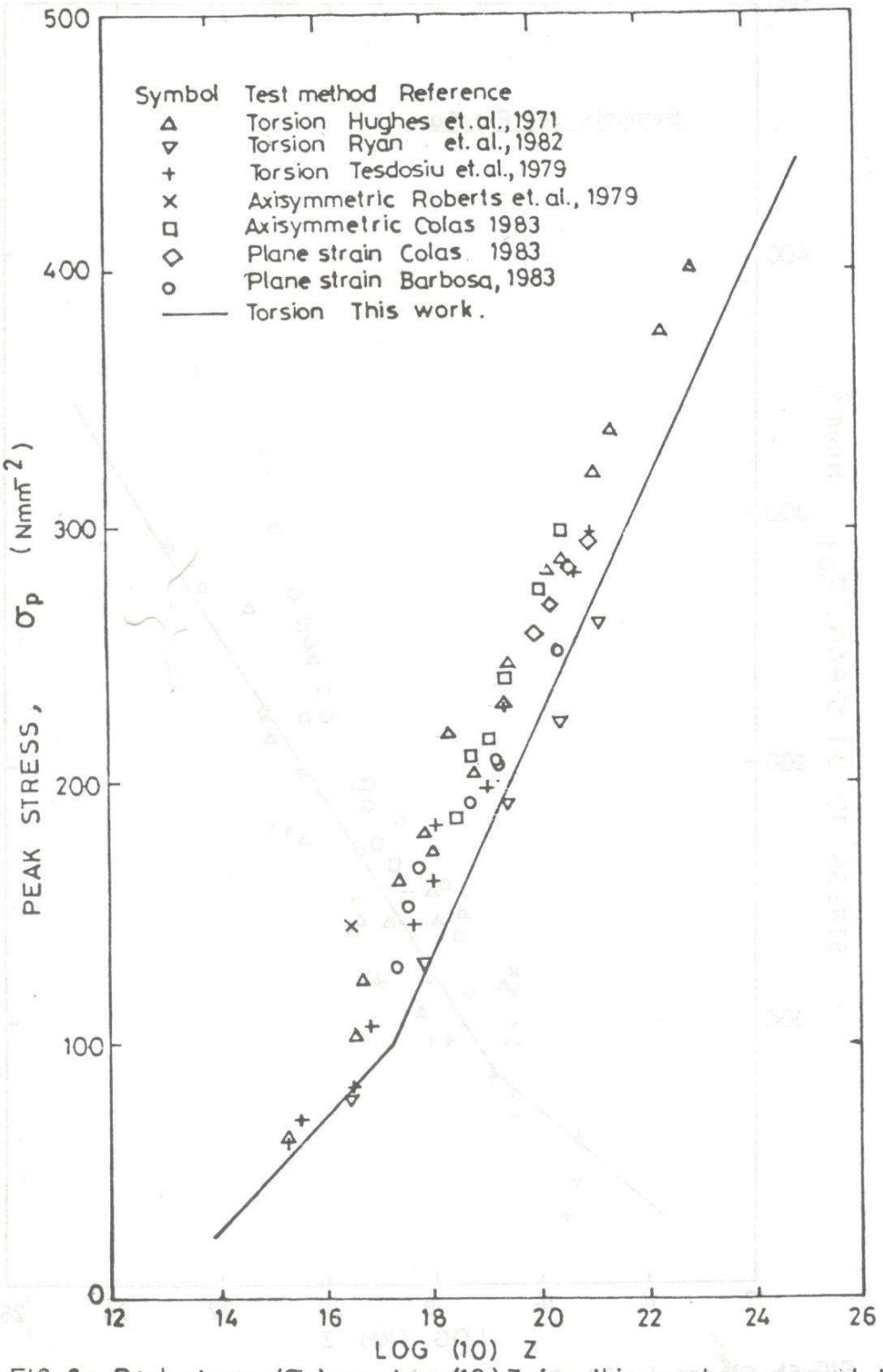


FIG. 6a. Peak stress (σ_p) vs Log (10) Z for this work compared to results on SS 316 by other researchers under different kinds of tests.

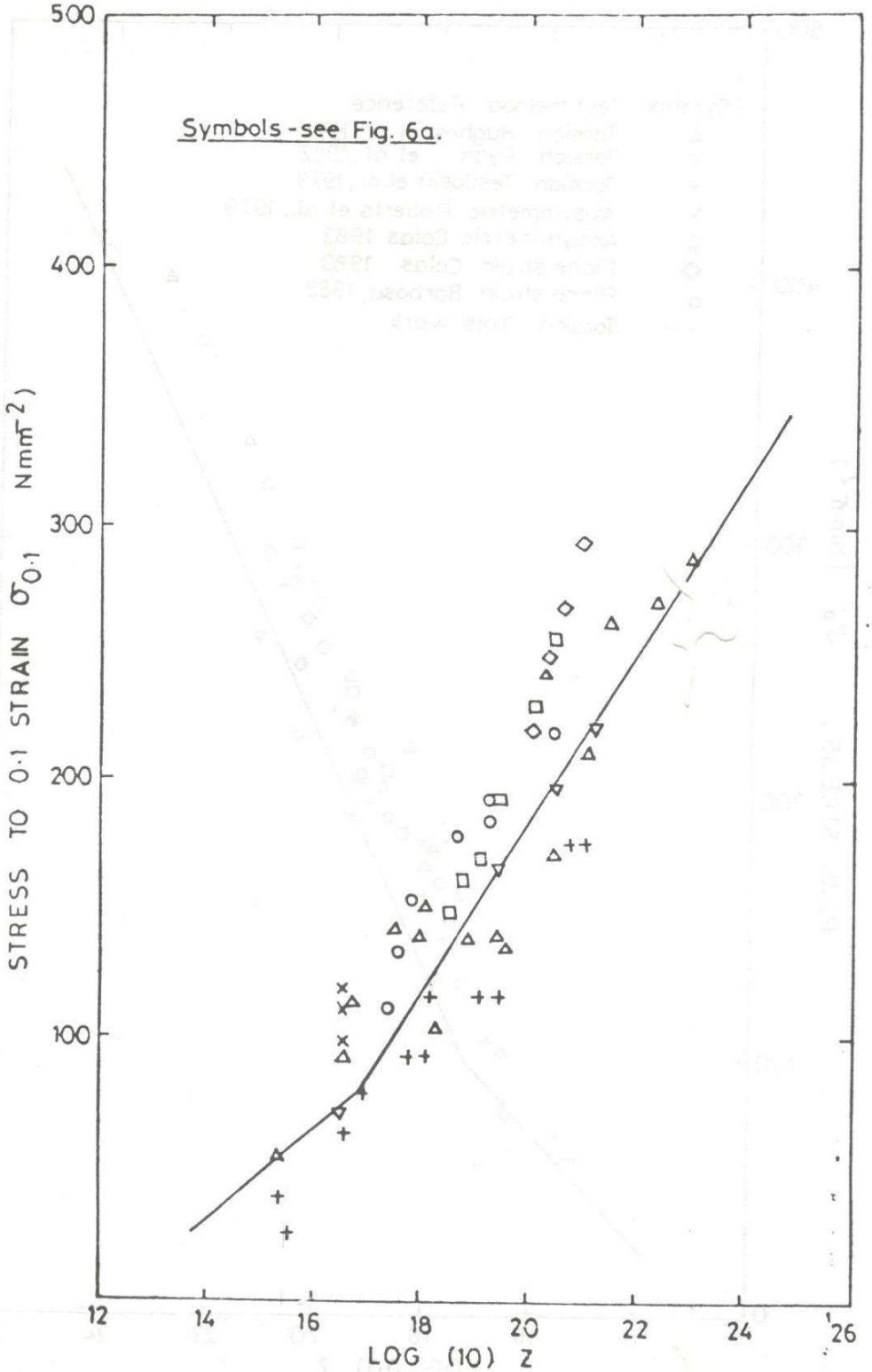


FIG. 6b. Stress to 0·1 strain ($\sigma_{0\cdot1}$) vs Log (10) Z for this work compared to results on SS 316 obtained by other researchers under different kinds of tests.

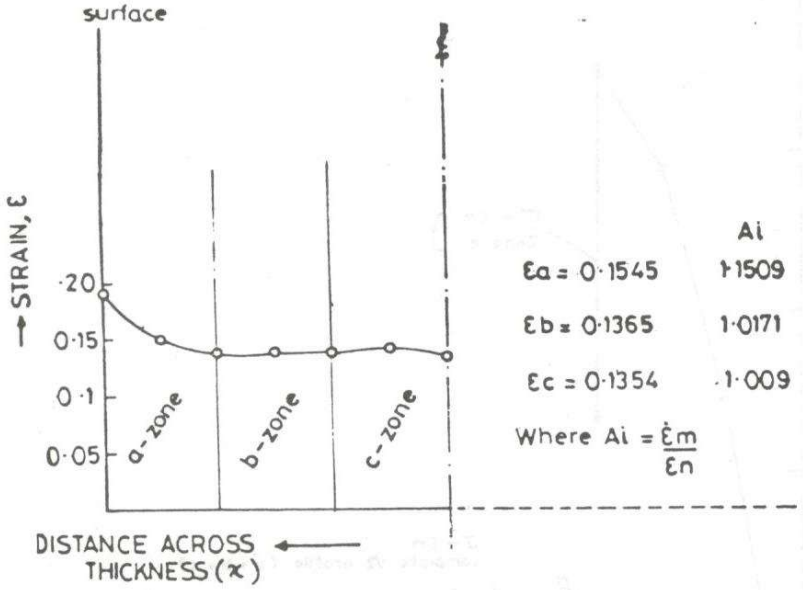


FIG. 7a. Strain profile across Zone a, b, c. of thickness.

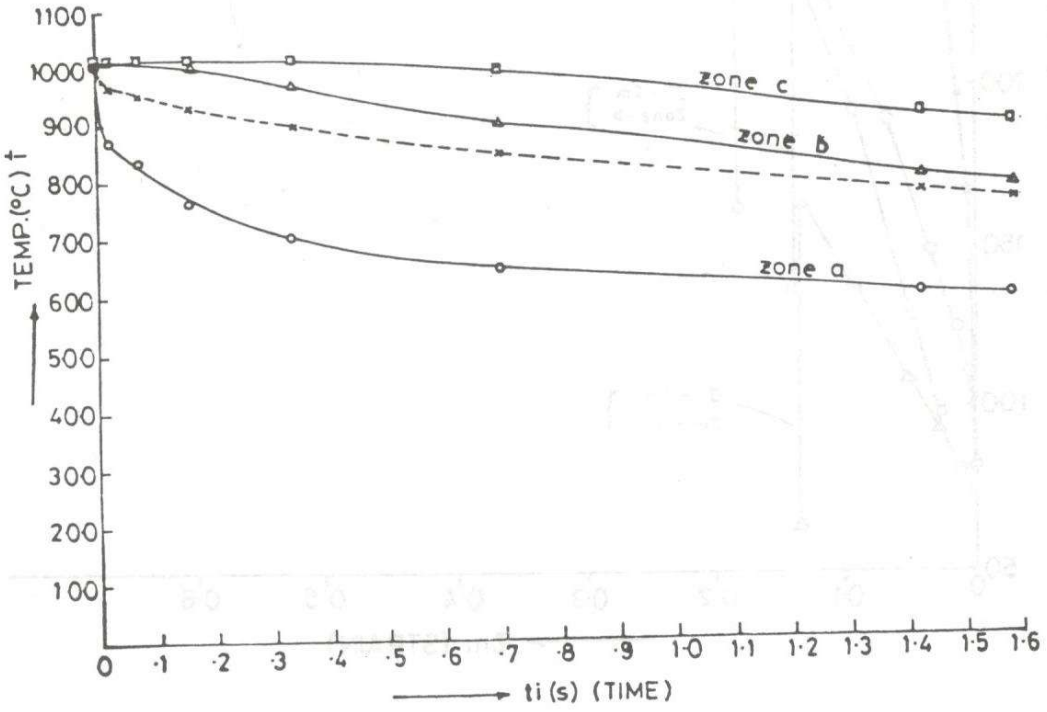


FIG. 7b. Temp. profile in Zone a, b, c. during roll contact.

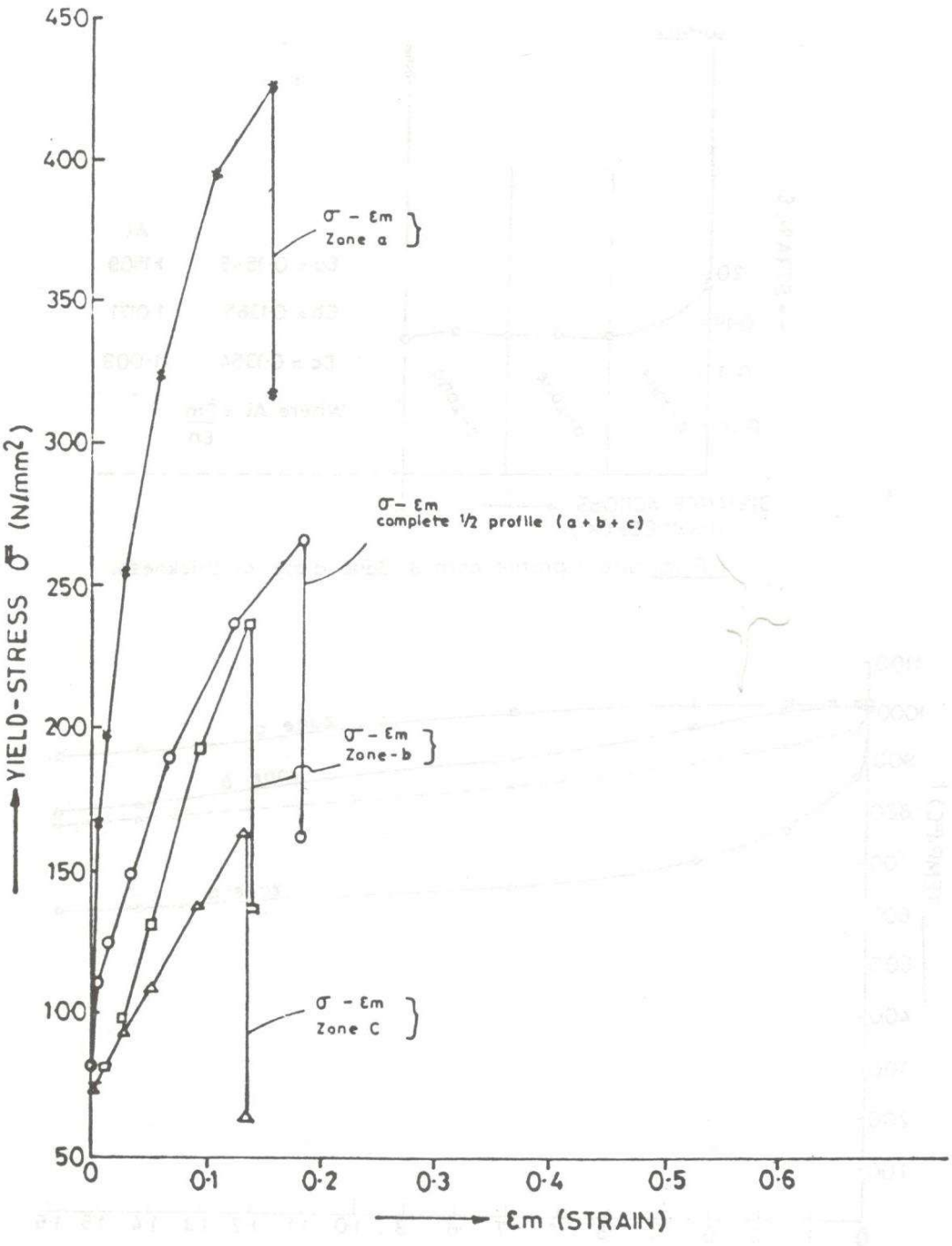


FIG. 8. Stress-strain (σ-εm) curves for zones a,b & c and for complete ½ profile of SP. PNI during roll contact.